UNIVERSITÀ DEGLI STUDI
DI GENOVA

Homework - 6

Department of Civil, Chemical and Environmental Engineering
Course: Turbulence and CFD Models

Submitted To:
Joel Guerrero

Submitted By :
Biniyam Sishah

Genoa, Italy

1 Introduction

This paper describes the mathematical and application scopes of the $\kappa - \kappa_L - \omega$ turbulence model Walters & Cokljat (2008). It's among turbulence models who's bases is the Boussinesq hypothesis. The model is a three equation model and is known to perform better for transition flows.

A critical examination of several turbulence models suggests that their ability to model transitional flows is an accidental artifact rather than reflection off any true predictive capacity. Methods for addressing boundary layer transition in computational fluid dynamics simulations can range from highly empirical approaches Where empirical approaches based on selecting an appropriate transition location and applying a fair balance model only downstream of this location to direct numerical simulation.

To predict transnational behavior of flows, RANS turbulent models use the common approaches of coupling fully turbulent models with empirical transition correlation and the addition of transport equations to the turbulence model equations to include the effects of transnational flow. The prior method is still an active area of research end presents problems for complex 3-dimensional geometries Greene & Hamilton (2006) and Kozulovic´ & Lapworth (2007). The more general approach makes use of additional transport equations or model terms to include the effect of transition on the flow field prediction.

One of the primary difficulties with implementing phenomenological modeling approach and one reason they are less prevalent than empirical models is that the physics of transition is still not entirely understood and indeed is an active area of research. Because of this some authors have argued that correlation-based models are more appropriate candidates for the consistent RANS-based transitions predictions than their physics-based counterparts. Menter et al. (2006) however recent analytical, numerical and experimental investigations have helped to highlight some of the universal characteristics of boundary layer flows, both transition and turbulent. Knowledge of the relevant scaling mechanism may allow reasonably accurate model forms without recourse to a purely empirical-based approach.

The model to be addressed here can be used to model laminar, translational, and turbulent flows in the framework of Reynolds averaging, in which the influence of unsteady velocity fluctuations on the mean flow is represented y the appearance of Reynolds stresses terms in the time-averaged governing equations. The Reynolds stress is typically interpreted as the "turbulent stress" also it is important to note that the Reynolds stress arises as a conse-

quences of the averaging processes and is nonzero for any time varying velocity field, even when the velocity fluctuations are not due to "turbulence" in the strict sense. In theory, transitional as well as turbulent fluctuations can be molded through the Reynolds stress tensor Wang & Perot (2002)steady laminar flow can be effectively "modeled" when the Reynolds stress components are assigned values that are negligibly small. The simplest RANS models assume a linear relationship between the Reynolds stress and the strain rate tensor, Boussinesq hypothesis:

$$\rho\overline{\mathbf{u}_i'\mathbf{u}_j'} - \frac{1}{3}\rho\overline{\mathbf{u}_k\mathbf{u}_k}\delta_{ij} = -2\mu_T S_{ij} \tag{1}$$

The primary advantage is its simplicity, but a major challenge lies in the fact that all the relevant scales' effects of the fluctuating velocity field must be modeled by the single parameter-the eddy viscosity. For the new model presented here this includes the physics of laminar-to-turbulent transition.

For the so called two transport equation models, two additional transport equations are solved to obtain the turbulence quantities used to compute the eddy viscosity. In the present model, an additional transport equation is included to represent pretransition (i.e. nonturbulent) velocity fluctuations.

Transition sensitivity modeling concept

The pretransition boundary layer is effectively laminar in terms of the mean velocity profile. As the freestream turbulence intensity increase, the mean velocity in this layer tends to become noticeably distorted. This shift in mean velocity profile is accomplished by development of relatively high amplitude streamwise fluctuations, which can reach intensities several times the freestream level Klebanoff (1971). This process leads to augmentation of skin friction and heat transfer and eventually leads to transition through the breakdown of the streamwise fluctuations. This process in known as bypass transition. It is important to not these streamwise fluctuations represent Klebanoff modes Klebanoff (1971) and are not turbulent in the usual sense.Mayle & Schulz (1997) developed the laminar kinetic energy concept to describe the development of pretranslational fluctuations leading to bypass transition. The energy of the fluctuations is referred to here as laminar kinetic energy (κ_L).

The dynamics of laminar kinetic energy production are not entirely understood at present. But two aspects are critical: selectivity of the boundary layer to certain free stream scales and amplification of low frequency disturbances in the boundary layer by the mean shear.

The growth of ($\kappa_L l$) has been shown to correlate with low-frequency normal(u') fluctuations of the free stream turbulence.

Mayle & Schulz (1997) has suggested that the growth of laminar kinetic energy was due to the transport of energy from the free stream in the boundary layer due to the pressure diffusion term in the kinetic energy budget. An alternative description were the growth in laminar kinetic energy is associated to the interaction of the Reynold stresses associated with pretranslational velocity fluctuations and the mean shear has gain traction recently due to a validation case Lardeau et al. (2007)using a large eddy simulation of the translational boundary layer.

The transition process itself is represented in the new model by a transfer of energy from the laminar kinetic energy (κ_L) the turbulent kinetic energy (κ_T).

Model equation

For ease of presenting the flow under consideration here is incompressible, with no body force, governed by the steady Reynolds-averaged continuity and momentum equations and a linear eddy-viscosity model is adopted for the Reynolds stresses.

Three equation model transport equations are solved for the turbulent kinetic energy (κ_T), the laminar kinetic energy (κ_L) and the scale -determining variable ω defined here as $\omega = \dfrac{\epsilon}{\kappa t}$ where ϵ is the isotropic dissipation.

$$\frac{D\kappa_T}{Dt} = P_{K_T} + R_{BP} + R_{NAT} - \omega\kappa_T - D_T + \frac{\partial}{\partial \mathbf{x}_j}\left[\left(\nu + \frac{\sigma_T}{\sigma_K}\right)\frac{\partial \kappa_T}{\partial \mathbf{x}_j}\right] \tag{2}$$

$$\frac{D\kappa_L}{Dt} = P_{K_L} + R_{BP} + R_{NAT} - D_L + \frac{\partial}{\partial \mathbf{x}_j}\left[\nu\frac{\partial \kappa_L}{\partial \mathbf{x}_j}\right] \tag{3}$$

$$\begin{aligned}\frac{D\omega}{Dt} =& C_{\omega l}\frac{\omega}{\kappa_T}P_{k_T} + \left(\frac{C_{wR}}{f_w} - 1\right)\frac{\omega}{\kappa_T}(R_{BP} + R_{NAT}) - C_{w2}\omega^2 \\ &+ C_{w3}f_w\sigma_T f^2\omega\frac{\sqrt{\kappa_T}}{d^3} + \frac{\partial}{\partial \mathbf{x}_j}\left[\left(\nu + \frac{\sigma_T}{\sigma_w}\right)\frac{\partial \omega_T}{\partial \mathbf{x}_j}\right]\end{aligned} \tag{4}$$

The various terms in the model equations represent production, destruction, and transport mechanisms.In the ω equation, the fully turbulent production, destruction, and gradient transport terms (first, third, and fifth terms on the right-hand side of Eq. (4)) are analogous to the similar terms in the κ_T and κ_L equations and are similar to terms that appear in

other $\kappa - \omega$ models forms.The transition production term (second term on right-hand side) is intended to produce a reduction in turbulence length scale during the transition breakdown process.The fourth term on the right-hand side was included in order to decrease the length scale in the outer region of the turbulent boundary layer, which is necessary to ensure correct prediction of the boundary layer wake region Walters & Leylek (2005).

The total fluctuation kinetic energy is $k_{TOT} = k_T + k_L$. The production of turbulent and laminar kinetic energy by mean strain is modeled as:

$$P_{k_T} = \nu_{T,s} S^2 \tag{5}$$

$$P_{k_L} = \nu_{T,l} S^2 \tag{6}$$

The "small-scale" eddy-viscosity concept follows Ref. 17, and is defined as

$$\nu_{T,s} = f_w f_{INT} C_\mu \sqrt{\kappa_{T,s}} \lambda_{eff} \tag{7}$$

where κ_T is the effective small-scale turbulence.

$$\kappa_{T,s} = f_{SS} f_w \kappa_T \tag{8}$$

The kinematic wall effect is included through an effective (wall limited) turbulence length scale λ_{eff} and damping function f_w Walters & Leylek (2004).

$$\lambda_{eff} = min(C_\lambda d, \lambda_T) \tag{9}$$

$$\lambda_T = \frac{\sqrt{\kappa_T}}{\omega} \tag{10}$$

$$f_w = \left(\frac{\lambda_{eff}}{\lambda_T} \right) \tag{11}$$

The viscous wall effect is incorporated through the viscous damping function, which is computed in terms of the effective turbulence Reynolds number.

$$f_\nu = 1 - exp\left(-\frac{\sqrt{Re_T}}{A_\nu} \right) \tag{12}$$

$$Re_T = \frac{{f^2}_w \kappa_T}{\nu \omega} \tag{13}$$

shear-sheltering effect is included in the damping function f_{SS}.

$$f_{SS} = exp\left[-\left(\frac{C_{SS}\nu\Omega}{\kappa_T}\right)^2\right] \tag{14}$$

The turbulent viscosity coefficient C is defined to satisfy the realizability constraint following Walters & Leylek (2004):

$$C_\mu = \frac{1}{A_0 + A_S\left(\frac{S}{\omega}\right)} \tag{15}$$

The effect of intermittency on the turbulence production is included through an empirical intermittency damping function.

$$f_{INT} = min\left(\frac{K_L}{C_{INT}\kappa_{ToT}}, 1\right) \tag{16}$$

The production of laminar kinetic energy κ_L is assumed to be governed by the large-scale near-wall turbulent fluctuations Walters & Leylek (2004), based on the correlation of pretransitional fluctuation growth with freestream low-frequency wall-normal turbulent fluctuations Volino & Simon (1997) and Leib et al. (1999). The large-scale turbulence contribution is

$$\kappa_{T,l} = \kappa_T - \kappa_{T,s} \tag{17}$$

Where the small contribution is defined by Eq. (8). The production term is

$$P_{\kappa_L} = \nu_{T,l}S^2 \tag{18}$$

where

$$\nu_{T,l} = min\left\{f_{\tau,l}C_{11}\left(\frac{\Omega\lambda_{eff}{}^2}{\nu}\right)\sqrt{\kappa_{T,l}}\lambda_{eff} + \beta_{TS}C_{12}Re_\Omega d^2\Omega, \frac{0.5(\kappa_L + \kappa_{T,1})}{S}\right\} \tag{19}$$

The limit is applied to ensure satisfaction of the realizability constraint for the total Reynolds stress contribution. The production term is comprised of two parts—the first addresses the development of Klebanoff modes and the second addresses self-excited (i.e., natural) modes This term is identical to the form proposed in Walters & Leylek (2004), with

$$Re_\Omega = \frac{d^2\Omega}{\nu} \tag{20}$$

$$\beta_{TS} = 1 - exp\left(-\frac{max(Re_\Omega - C_{TS,crit}0)^2}{A_{TS}}\right) \tag{21}$$

$$f_{\tau,1} = 1 - exp\left[-C_{\tau,l}\frac{\kappa_{T,l}}{\lambda_{eff}^2}\Omega^2\right] \tag{22}$$

The anisotropic near-wall dissipation terms for κ_T and κ_L take a common form.

$$D_T = \nu\frac{\partial\sqrt{\kappa_T}}{\partial \mathbf{x}_j}\frac{\partial\sqrt{\kappa_T}}{\partial \mathbf{x}_j} \tag{23}$$

$$D_L = \nu\frac{\partial\sqrt{\kappa_L}}{\partial \mathbf{x}_j}\frac{\partial\sqrt{\kappa_L}}{\partial \mathbf{x}_j} \tag{24}$$

The turbulent transport terms in the κ_T and ω equations include an effective diffusivity α_T defined as

$$\alpha_T = f_\nu C_{\mu,std}\sqrt{\kappa_{T,s}}\lambda_{eff} \tag{25}$$

The boundary layer production term intended to reproduce proper behavior of the boundary layer wake region includes a kinematic damping function of the form

$$f_w = 1 - exp\left[-0.41\left(\frac{\lambda_{eff}}{\lambda_T}\right)^4\right] \tag{26}$$

The remaining terms in the transport equations are related to the laminar-to-turbulent transition mechanism in the model. As mentioned above, transition occurs as a transfer of energy from κ_L to κ_T, with a concurrent reduction in turbulence length scale from the freestream value to the value found in an equilibrium turbulent boundary layer. The model terms R_{BP} and R_{NAT} appear with opposite signs in the κ_L and κ_T equations and represent bypass and natural transition, respectively. The model forms are

$$R_{BP} = \frac{C_R\beta_{BP}\kappa_L\omega}{f_w} \tag{27}$$

$$R_{NAT} = C_{R,NAT}\beta_{NAT}\kappa_L\Omega \tag{28}$$

Transition initiation is governed by the threshold functions β_{BP} and β_{NAT} As discussed in the previous section, transition in both cases is assumed to initiate when the characteristic time-scale for turbulence production is smaller than the viscous diffusion timescale of the pretransitional fluctuations. The forms used are

$$\beta_{BP} = 1 - exp\left(-\frac{\phi_{BP}}{A_{BP}}\right) \tag{29}$$

$$\phi_{BP} = max\left[\left(\frac{\kappa_T}{\nu\Omega} - C_{BP,crit}\right), 0\right] \tag{30}$$

$$\beta_{NAt} = 1 - exp\left(-\frac{\phi_{NAT}}{A_{NAT}}\right) \tag{31}$$

$$\phi_{NAT} = max[(Re_{\Omega} - \frac{C_{NAT,crit}}{f_{NAT,crit}}), 0] \tag{32}$$

$$f_{NAT,crit} = 1 - exp\left(-C_{NC}\frac{\sqrt{\kappa_L}\bar{d}}{\nu}\right) \tag{33}$$

Note that the function $f_{NAT,crit}$ is included so that the amplitude of the pretransitional fluctuations influences the initiation of natural transition in an appropriate manner. The turbulent viscosity used in the momentum equations is the sum of the small-scale and large-scale contributions defined above.

Table 1: Summary of model constants

A_0=4.04	C_{INT}=0.75	$C_{\omega 1}$=0.44
A_s=2.12	$C_{TS,crit}$=1000	$C_{\omega 2}$=0.92
A_v=6.75	$C_{R,NAT}$=0.02	$C_{\omega 3}$=0.3
A_{BP}=0.6	C_{l1}=3.4*10^{-6}	$C_{\omega R}$=1.5
A_{NAT}=200	C_{l2}=1.0*10^{-10}	C_{λ}=2.495
A_{TS}=200	C_R=0.12	$C_{\mu,std}$=0.09
$C_{BP,crit}$=1.2	$C_{\alpha,\theta}$=0.035	Pr_{θ}=0.85
C_{NC}=0.1	C_{SS}=1.5	σ_k=1
$C_{NAT,crit}$=1250	$C_{\tau,l}$=4360	σ_{ω}=1.17

$$\nu_T = \nu_{T,s} + \nu_{T,l} \tag{34}$$

When including heat transfer effects, the turbulent heat flux vector can be modeled using a turbulent thermal diffusivity α_θ

$$-\overline{u_i T} = \alpha_\theta \frac{\partial T}{\partial \mathbf{x}_j} \tag{35}$$

$$\alpha_\theta = f_w \left(\frac{\kappa_T}{\kappa_{TOT}} \right) \frac{\nu_{T,s}}{Pr_\theta} + (1 - f_w) C_{\alpha,\theta} \sqrt{\kappa_T} \lambda_{eff} \tag{36}$$

1.1 Boundary conditions

The boundary conditions are similar to those for more commonly used RANS turbulent models. At solid boundaries, the no-slip condition enforces

$$\kappa_T = \kappa_L = 0 \tag{37}$$

A zero-normal gradient condition is used for ω

$$\frac{\partial \omega}{\partial \eta} \tag{38}$$

where η is the wall-normal coordinate direction. Note that the wall boundary condition Eq. (38) is substantially different from that commonly used in other model forms. At flow inlets, the values of κ_T and ω are prescribed exactly analogous to other two-equation models. The turbulent kinetic energy is often determined based on the inlet turbulence intensity Tu_∞, assuming isotropic freestream turbulence:

$$Tu - \infty = \frac{\sqrt{\frac{2}{3}\kappa_T}}{U_\infty} \tag{39}$$

The value of the specific dissipation is chosen to coincide with the available freestream information. For example, if the turbulent length scale or the decay rate is known, may be chosen to reproduce the appropriate freestream conditions. For velocity inlets sufficiently far from solid walls, the inlet flow may be considered to be completely outside the boundary layer. In that case, the laminar kinetic energy associated with pretransitional fluctuations is zero. The appropriate inlet boundary condition is therefore κ_L=0.

1.2 Validation cases

All of the simulations presented here were performed using the FLUENT solver, version 6.4.All results presented in this study used a second order upwind-based discretization scheme.

For all test case geometries, an initial mesh was constructed with a first cell y+ value of one or less, and a structured body fitted mesh in the boundary layer region. In order to confirm grid independence of the results, a second mesh with twice the resolution in the streamwise and wall-normal directions was constructed, and the results were compared to the original mesh. In all cases, the results showed negligible difference and were therefore judged to be mesh independent. All cases were run to full convergence, determined based on a drop in residuals of typically five orders of magnitude, as well as a flattening of all residuals indicating that machine accuracy had been reached.

1.2.1 Fully Developed Turbulent Channel Flow

The first test case is intended to verify the correct behavior of the new model in the fully-turbulent regime. The test case is a fully developed 2D channel flow with Re_T=395, and the results are compared to the DNS simulations of Moser et al. (1999).

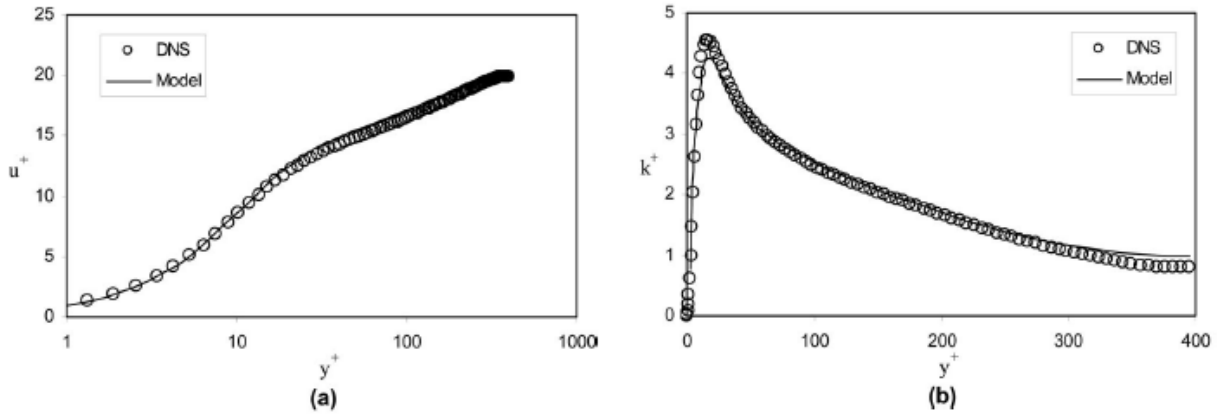

Figure 1: Dimensionless velocity (a) and turbulent kinetic energy (b) profiles for fully developed turbulent channel flow at Re_T= 395

Figure 1 (a) shows the dimensionless velocity profile in the channel expressed in terms of inner scaling. The new model indicates good agreement with the DNS data, including a clear reproduction of the viscous sublayer, buffer zone, and inertial sublayer. Figure1 (b) shows the turbulent kinetic energy profile in the channel. The new model correctly reproduces the peak

in turbulence near y+=15, although the magnitude is underpredicted slightly. Throughout most of the channel extent, the model is in excellent agreement with the DNS data.

1.2.2 Zero-Pressure-Gradient Flat Plate

The transition behavior of the model was tested for a simple zero-pressure-gradient (ZPG) flat plate, in order to assess the response to freestream turbulence, and to compare the prediction of transition start length with experimental data and available empirical correlations.

The test cases chosen match the T3A, T3B, and T3A validation cases from the European Research Consortium on Flow, Turbulence and Combustion (ERCOFTAC) database.

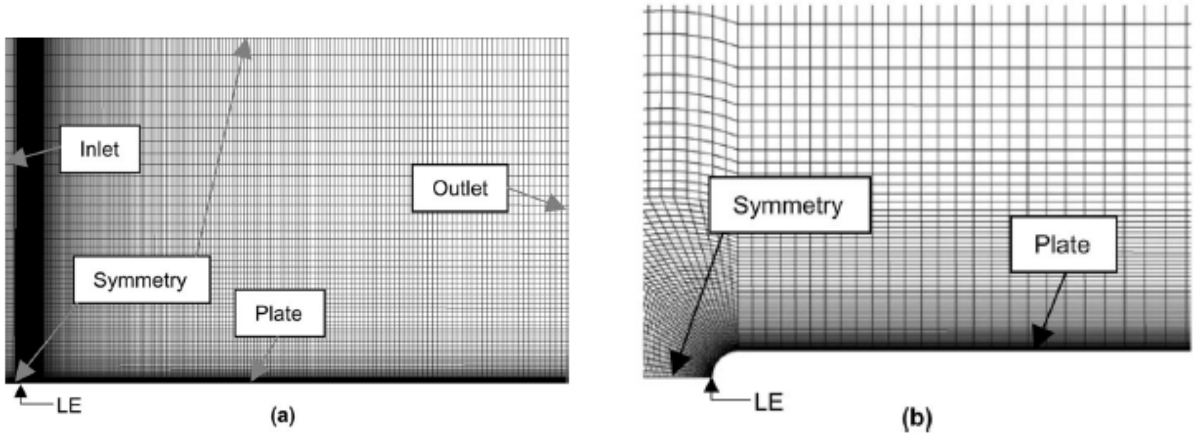

Figure 2: Domain and computational meshes used for ZPG flat plate test cases: (a) overall mesh; and (b) close-up view of leading-edge region

Case	Tu (%)	μ_T/μ
T3A–	0.874	8.73
T3A	3.3	12.0
T3B	6.5	100.0

The predicted skin friction coefficient is shown in Figure **??** for cases T3A, T3A, and T3B. The figure also indicates the limiting cases of laminar and turbulent flows on the flat plate. The model yields a good agreement between the experimental data for all three cases.

1.2.3 Airfoil Test Case

One example of a realistic geometry for which transition is often an important factor is flow over airfoils. The new model has been applied to a number of airfoil test cases in order to

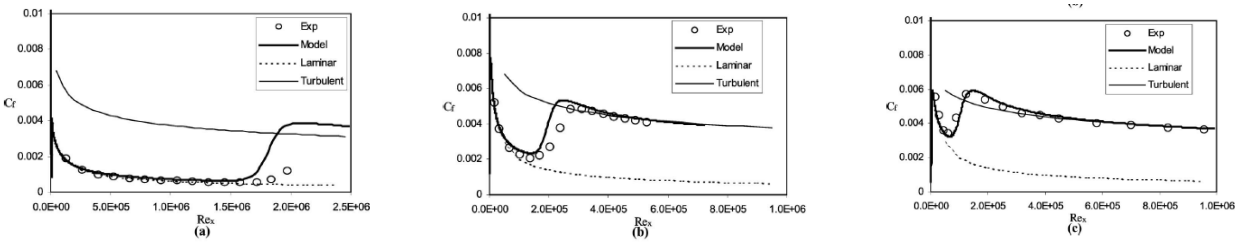

Figure 3: Distribution of skin friction coefficient for ZPG flat plate cases:(a) T3A, (b) T3A, and, (c). T3B

assess predictive capability in terms of wall shear stress and heat transfer rates.

The airfoil case chosen here for presentation is that of the Aerospatiale A-airfoil configuration at Reynolds number (based on chord length) of 2 x 10^6, Mach number of 0.15, and angle of attack (α) of 13.3 deg. This configuration has been well studied, both experimentally Haase et al. (2013) and numerically Schmidt & Thiele (2003) and is known to exhibit complex boundary layer transition and separation behavior.

The airfoil geometry and mesh are illustrated in Figure 4, left, The mesh used was 2D structured C-type with a total of 65,000 cells. The inlet turbulence intensity for the simulations was 0.2, and the turbulent viscosity ratio was 10.

CFD results were compared to experimental data in terms of skin friction coefficient on the upper suction surface and are shown in Figure 4, right, The reported experimental data indicate that transition occurs on the suction surface at s/C=0.12. It is apparent in the figure that this transition location is well predicted by the model, and a fully-turbulent boundary layer is indicated downstream of this location.

1.3 Summary

The $\kappa - \kappa_L - \omega$ RANS based turbulent model uses a physics-based (i.e., phenomenological) eddy-viscosity modeling approach based on the addition of one transport equation to a simple $\kappa - \omega$ model framework. The additional transport equation represents the effects of pretransitional fluctuations, including Klebanoff modes and Tollmien–Schlichting waves that are the precursors to bypass and natural transition, respectively

The model results presented here show a dramatic improvement over traditional fully-turbulent models, without the need for empirical correlations or user prescribed transition information. While no simple modeling methodology will ever yield perfect predictive capa-

bility, these results suggest that the physics-based approach adopted here allows designers to significantly extend RANS-based computational analysis capability by providing realistic transitional modeling capability in a relatively simple eddyviscosity framework.

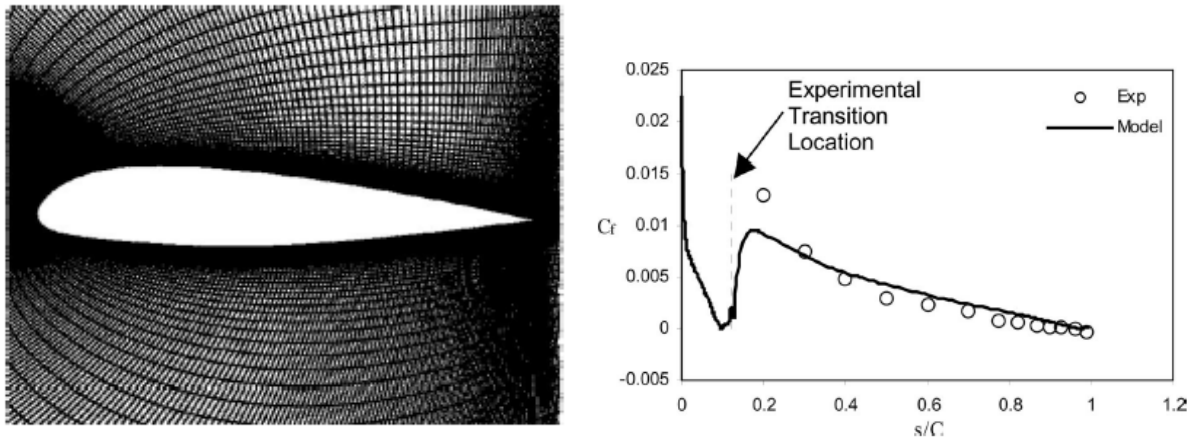

Figure 4: A-airfoil test case: Structured C-type 2D mesh (**left**), Comparison of predicted and measured skin friction coefficients (**right**)

Nomenclature

C = airfoil chord length
C_μ = turbulent viscosity coefficient
d = wall distance
D_T = anisotropic (near-wall) dissipation term for k_T
D_L = anisotropic (near-wall) dissipation term for k_L
f_{INT} = intermittency damping function
$f_{\mathrm{NAT,crit}}$ = model function incorporating freestream turbulence effects on natural transition
f_W = inviscid near-wall damping function
f_{SS} = shear-sheltering damping function
f_v = viscous near-wall damping function
f_ω = boundary layer wake term damping function in ω equation
$f_{\tau,l}$ = time-scale damping function
h = heat transfer coefficient
k_L = laminar kinetic energy
k_T = turbulent kinetic energy
$k_{T,l}$ = effective "large-scale" turbulent kinetic energy
$k_{T,s}$ = effective small-scale turbulent kinetic energy
k_{TOT} = total fluctuation kinetic energy, k_T+k_L
P_{kL} = production of laminar kinetic energy by mean strain rate
P_{kT} = production of turbulent kinetic energy by mean strain rate
Pr_θ = turbulent Prandtl number
R_{BP} = bypass transition production term
R_{NAT} = natural transition production term
Re_θ = momentum thickness Reynolds number
Re_T = turbulence Reynolds number
Re_τ = Reynolds number based on friction velocity and channel half-height
Re_x = local Reynolds number
Re_Ω = vorticity-based Reynolds number
S = magnitude of mean strain rate tensor
S_{ij} = strain rate tensor
s = distance along the airfoil surface (from the stagnation point)
T = temperature
t = time
Tu_∞ = freestream turbulence intensity
U_∞ = freestream mean velocity
u_i = velocity vector
v' = wall-normal freestream turbulence fluctuation magnitude
x = downstream distance
x_i = position vector
y^+ = wall distance normalized by inner scaling
α = thermal diffusivity
α_θ = turbulent thermal diffusivity
α_T = effective diffusivity for turbulence dependent variables
β_{BP} = bypass transition threshold function
β_{TS} = Tollmien–Schlichting threshold function
β_{NAT} = natural transition threshold function
δ = 99% boundary layer thickness
δ_{ij} = Kronecker delta
ε = farfield isotropic dissipation rate
φ_{BP} = model bypass transition parameter
φ_{NAT} = model natural transition parameter
η = wall-normal coordinate direction
λ_{eff} = effective (wall-limited) turbulence length scale
λ_T = turbulent length scale
ν = kinematic viscosity
ν_T = turbulent kinematic viscosity
$\nu_{T,s}$ = small-scale turbulent viscosity contribution
$\nu_{T,l}$ = large-scale turbulent viscosity contribution
Ω = magnitude of mean rotation rate tensor
ω = inverse turbulent time-scale
θ = boundary layer momentum thickness
ρ = density
μ = dynamic viscosity
μ_T = turbulent or "eddy"-viscosity

References

Greene, F., & Hamilton, H. (2006). Development of a boundary layer properties interpolation tool in support of orbiter return to flight. In *9th aiaa/asme joint thermophysics and heat transfer conference* (p. 2920).

Haase, W., Brandsma, F., Elsholz, E., Leschziner, M., & Schwamborn, D. (2013). *Euroval—an european initiative on validation of cfd codes: Results of the ec/brite-euram project euroval, 1990–1992* (Vol. 42). Springer-Verlag.

Klebanoff, P. (1971). Effect of free-stream turbulence on a laminar boundary layer. In *Bulletin of the american physical society* (Vol. 16, pp. 1323–+).

Kozulovic´, D., & Lapworth, B. (2007). An approach for inclusion of a non-local transition model in a parallel unstructured cfd code. In *Fluids engineering division summer meeting* (Vol. 42886, pp. 83–92).

Lardeau, S., Li, N., & Leschziner, M. A. (2007). Large eddy simulation of transitional boundary layers at high free-stream turbulence intensity and implications for rans modeling.

Leib, S., Wundrow, D. W., & Goldstein, M. (1999). Effect of free-stream turbulence and other vortical disturbances on a laminar boundary layer. *Journal of Fluid Mechanics*, *380*, 169–203.

Mayle, R., & Schulz, A. (1997). Heat transfer committee and turbomachinery committee best paper of 1996 award: The path to predicting bypass transition.

Menter, F., Langtry, R., & Völker, S. (2006). Transition modelling for general purpose cfd codes. *Flow, turbulence and combustion*, *77*(1-4), 277–303.

Moser, R. D., Kim, J., & Mansour, N. N. (1999). Direct numerical simulation of turbulent channel flow up to re τ= 590. *Physics of fluids*, *11*(4), 943–945.

Schmidt, S., & Thiele, F. (2003). Detached eddy simulation of flow around a-airfoil. *Flow, turbulence and combustion*, *71*(1-4), 261–278.

Volino, R., & Simon, T. (1997). Boundary layer transition under high free-stream turbulence and strong acceleration conditions: part 2—turbulent transport results.

Walters, D. K., & Cokljat, D. (2008). A three-equation eddy-viscosity model for reynolds-averaged navier–stokes simulations of transitional flow. *Journal of fluids engineering*, *130*(12).

Walters, D. K., & Leylek, J. H. (2004). A new model for boundary layer transition using a single-point rans approach. *J. Turbomach.*, *126*(1), 193–202.

Walters, D. K., & Leylek, J. H. (2005). Computational fluid dynamics study of wake-induced transition on a compressor-like flat plate. *J. Turbomach.*, *127*(1), 52–63.

Wang, C., & Perot, B. (2002). Prediction of turbulent transition in boundary layers using the turbulent potential model. *Journal of Turbulence*, *3*(1), 1–15.